Research Square

Preprints are preliminary reports that have not undergone peer review.
They should not be considered conclusive, used to inform clinical practice,
or referenced by the media as validated information.

Synergistic effects of urine-derived stem cells and platelet lysate on urethral sphincter regeneration in a rat model of pudendal nerve injury

Eun Hye Lee
Kyungpook National University
Minji Jeon
Kyungpook National University Hospital
Jun-Koo Kang
Kyungpook National University
Jae-Wook Chung
Kyungpook National University
Yun-Sok Ha
Kyungpook National University
Phil Hyun Song
Yeungnam University College of Medicine
Man-Hoon Han
Kyungpook National University
Tae Gyun Kwon
Kyungpook National University
Bum Soo Kim
urokbs@knu.ac.kr

Kyungpook National University

Research Article

Keywords: stem cells, incontinence, platelet, urethral sphincter, rat

Posted Date: November 1st, 2026

DOI: https://doi.org/10.21203/rs.3.rs-10687734/v1

License: This work is licensed under a Creative Commons Attribution 4.0 International License.
Read Full License

Additional Declarations: No competing interests reported.

Abstract

Background

Stress urinary incontinence (SUI) results from urethral sphincter insufficiency. Urine-derived stem cells (USCs) possess myogenic and neurotrophic potential, while platelet lysate (PL), enriched with PDGF, VEGF, TGF-β1, and EGF, enhances stem cell proliferation and engraftment. This study comprehensively evaluated the therapeutic efficacy of USCs alone, PL alone, and their combination in a pudendal nerve injury (PNI)-induced rat model of SUI.

Methods

Thirty female Sprague–Dawley rats were assigned to five groups (n = 6): Ctrl, PNI, PNI+Cell, PNI + PL, and PNI+Cell + PL. One week after surgical PNI induction, 1 × 10^5 USCs in PBS, PBS with 10% PL, or USCs in PBS with 10% PL were injected into the external urethral sphincter. Conscious urodynamic studies assessed leak point pressure (LPP) and closing pressure (CP) at days 3, 7, and 14. Urethral sphincteric tissues were analyzed by H&E, Masson's trichrome, immunohistochemistry (nAChRα1, α-SMA, neurofilament), and quantitative PCR for myogenic (Pax7, MyoD, Myogenin, Mef2) and neuronal markers (GFAP, β-tubulin III, Neurofilament, MAP2).

Results

PNI significantly reduced LPP and CP. The PNI+Cell + PL group demonstrated the greatest functional recovery, with LPP approaching control levels at day 14. Combined treatment most effectively upregulated myogenic and neuronal markers, normalized MyoD expression, preserved muscle architecture, reduced fibrosis, and restored nAChRα1, α-SMA, and neurofilament expression compared with either monotherapy.

Conclusions

USC and PL combination therapy synergistically restored urethral sphincter function and promoted neuromuscular regeneration superior to either treatment alone, representing a promising regenerative strategy for SUI.

Background

Stress urinary incontinence (SUI) is a highly prevalent condition characterized by the involuntary leakage of urine during activities that increase intra-abdominal pressure, such as coughing, sneezing, or physical exertion [1]. The etiology of SUI is multifactorial, primarily involving the anatomical weakening of the pelvic floor musculature and the functional impairment of the external urethral sphincter (EUS). Current

conservative and surgical modalities for SUI, including pelvic floor muscle training, bulking agents, and mid-urethral sling procedures, predominantly aim to provide anatomical support or artificially increase outlet resistance [2]. Despite the high prevalence and significant quality-of-life burden associated with SUI, current treatment options remain limited. Conservative measures such as pelvic floor rehabilitation offer partial benefit, while surgical approaches including mid-urethral slings carry risks of mesh-related complications and do not address the underlying neuromuscular deficit [3]. These unmet clinical needs have fueled growing interest in regenerative medicine strategies targeting the neuromuscular pathology of sphincter dysfunction.

Mesenchymal stem cells (MSCs) derived from bone marrow, adipose tissue, amniotic fluid and muscle have demonstrated promising potential in preclinical SUI models [4]. However, their clinical translation is often hindered by invasive harvesting procedures, limited cellular yield, and age-dependent declines in proliferation and multilineage differentiation capabilities. In this context, urine-derived stem cells (USCs) have emerged as a highly attractive alternative [5]. USCs can be isolated non-invasively, continuously, and at low cost. Furthermore, USCs possess robust proliferative capacity, high telomerase activity, and a strong propensity to differentiate into myogenic, neurogenic, and endothelial lineages, making them uniquely suited for urologic tissue engineering [6]. USCs have also been demonstrated to express neurotrophin-related molecules including nerve growth factor (NGF) and brain-derived neurotrophic factor (BDNF), conferring neuroprotective effects in the injured sphincter microenvironment [7]. However, cell survival following transplantation into damaged tissue remains a critical barrier, as the hostile milieu —characterized by oxidative stress, inflammation, and reduced growth factor availability—substantially limits therapeutic efficacy [8].

To overcome this limitation, biological adjuvants are required to optimize the local niche [9]. Platelet lysate (PL), generated through the lysis of concentrated platelets, is a rich source of bioactive molecules, including platelet-derived growth factor (PDGF), vascular endothelial growth factor (VEGF), transforming growth factor-beta (TGF-β), and basic fibroblast growth factor (bFGF) [10]. These factors collectively promote cell proliferation, angiogenesis, extracellular matrix remodeling, and neural repair, rendering PL a highly versatile regenerative substrate [11]. Unlike platelet-rich plasma (PRP), PL undergoes complete platelet lysis, yielding a standardized, reproducible growth factor preparation free of viable cells and residual platelet membrane debris [12]. PL has been evaluated as a cell culture supplement capable of enhancing USC expansion and viability, as well as a direct injectable therapeutic in musculoskeletal and wound healing applications [13,14]. The potential of PL to create a pro-regenerative niche within injured sphincter tissue—augmenting USC survival, paracrine activity, and neurotrophic signaling—provides strong theoretical justification for combining USCs with PL in the treatment of pudendal nerve injury (PNI)-associated sphincter dysfunction. However, the combined application of USC and PL has not previously been evaluated in a PNI model.

We hypothesized that the co-administration of USCs and PL would exert a synergistic therapeutic effect, overcoming the poor cell survival associated with isolated cell therapy while maximizing neuromuscular regeneration. Therefore, the present study aims to evaluate the combined effects of human USCs and

human PL on urethral sphincter regeneration, utilizing functional, histological, and molecular assessments in a rat model of PNI-induced SUI.

Methods

Animal model

Thirty female Sprague–Dawley rats (6 weeks old; n = 6 per group) were purchased from Orient Bio (Sungnam, Republic of Korea) and randomly assigned to five experimental groups (Ctrl, PNI, PNI+Cell, PNI + PL, PNI+Cell + PL), and maintained in a pathogen-free, temperature- and humidity-controlled environment (22 ± 2°C, 50–60% relative humidity) with a 12-h light/dark cycle and free access to standard rodent chow and water, with appropriate bedding and environmental enrichment provided in accordance with the Guide for the Care and Use of Laboratory Animals. All procedures were approved by the Institutional Animal Care and Use Committee of Yeungnam University Medical Center (YUMC-AEC2024-010). Under inhalation anesthesia with isoflurane (2–3% in oxygen), bilateral pudendal nerve injury was surgically induced, a polyethylene catheter (PE-50; Becton Dickinson, USA) was implanted into the bladder dome, and after a week, treatments were administered into two distinct sites of the external urethral sphincter using a Hamilton microsyringe under aseptic conditions during the same surgical session. Depending on the experimental group, animals received either 1×10^5 cells suspended in phosphate-buffered saline (PBS), PBS supplemented with 10% platelet lysate (PL) without cells, or 1×10^5 cells suspended in PBS supplemented with 10% platelet lysate (10 μL per site; total 20 μL per animal). To minimize postoperative discomfort, buprenorphine (0.05 mg/kg, subcutaneously, every 12 h for 48 h) was administered as a standard analgesic regimen, and the animals were monitored daily for general health, surgical site condition, and signs of distress throughout the experimental period. Conscious urodynamic studies (UDS) were conducted at 3, 7, and 14 days after the surgical and injection procedures. At the 14-day endpoint, animals were euthanized by CO_2 inhalation followed by cervical dislocation, and urethral sphincter tissues were harvested for histological and molecular analyses. All animal experiments were conducted and reported in accordance with the ARRIVE guidelines 2.0.

Cell preparation (urine-derived stem cell)

For USC preparation, approximately 100 mL of freshly voided urine was obtained from a healthy male volunteer under sterile conditions after informed consent. The collected sample was immediately transported to the laboratory and centrifuged at 400 × g for 10 minutes at room temperature. The resulting cell pellet was carefully washed twice with PBS supplemented with 5% penicillin/streptomycin (P/S; Sigma-Aldrich, St. Louis, MO, USA) to minimize microbial contamination. After the final wash, the cells were resuspended and seeded into 12-well culture plates at a density of approximately 1,000 cells per well. Cells were cultured in a mixed medium consisting of keratinocyte serum-free medium and progenitor cell medium (Gibco, Carlsbad, CA, USA) at a 1:1 ratio, supplemented with growth factors

according to the manufacturer's recommendations. The plates were maintained at 37°C in a humidified atmosphere with 5% CO_2, and the medium was changed every 2–3 days until colonies appeared.

Platelet lysate preparation

Expired platelet units were obtained from the biobank of Kyungpook National University Hospital (Daegu, Korea) with prior approval from the institutional review board (KNUH 2019-08-008-002). Upon receipt, the samples were immediately stored at − 80°C until processing. For the 27 frozen units, thawing was performed by placing the vials in a 37°C water bath for 2 minutes with gentle agitation (30 rpm). Subsequently, 1.5 mL of each thawed sample was centrifuged at 13,000 rpm for 30 minutes at 4°C, and the resulting supernatant was filtered through a 0.22 μm low-protein binding filter (BD Falcon, Franklin Lakes, NJ, USA). The remaining thawed fractions were pooled, dispensed, and further centrifuged at 3,500 × g for 30 minutes at 4°C. The supernatant obtained from this step was clarified using a 40 μm cell strainer (BD Falcon) to remove residual particulates. All aliquots were stored at − 80°C until further use. Each preparation was carried out in triplicate, and all experiments were repeated three times.

Quantitative PCR

Urethra tissue samples were snap-frozen at − 80°C until further processing. Total RNA was isolated using the Maxwell® RSC SimplyRNA Cell Kit in Maxwell™ 16 instrument (Promega, Madison, WI, USA). RNA concentrations were quantified, and 1 μg of each sample was reverse-transcribed into complementary DNA (cDNA) with GoScript™ Reverse Transcriptase (Promega, Madison, WI, USA). Quantitative real-time PCR was then conducted on a StepOnePlus™ Real-Time PCR System (Applied Biosystems, Foster City, CA, USA). The primer sequences employed for amplification are summarized in Table 1.

Table 1
Primer sequences

Gene	Forward primer (5' → 3')	Reverse primer (5' → 3')
β-tubulin	TGG AGA ACA CGG ATG AGA CC	GAA TCG AAG GGA GGT GGT GA
GAPDH	AAG ATG GTG AAG GTC GGT GT	TGA CTG TGC CGT TGA ACT TG
GFAP	TAA GCT AGC CCT GGA CAT CG	TAC AGG AAT GGT GAT GAG GT
MAP2	TCT CAG TTC AGT GCC AGA GG	TTT CCT GAG GTG CTT CGG AT
Mef2	TCA GTT GGG AGC TTG CAC TA	TGG TGG TAC GGT CTC TAG GA
MyoD	GGG AAG GGA AGA GCA GAA GT	CTG GCC ACT CAA AGA TCA GC
Myogenin	CCA GTG AAT GCA ACT CCC AC	GCG AGC AAA TGA TCT CCT GG
Neurofilament	GCT AAA GAG AAG AAG GCG GC	CAC CTC CTC CTT CTT CGG TT
Pax7	TGG GTT ACG AAT TCC AGC CT	CCT ACC CTC TTG CTT CCC AA

Histological analysis

For histological evaluation, urethra specimens were fixed in 4% neutral-buffered formalin. Following fixation, tissues were paraffin-embedded to generate blocks and subsequently sectioned into 5-μm slices for hematoxylin and eosin (H&E), Masson's trichrome, and immunohistochemical (IHC) staining. Antigen retrieval was performed by heating the sections in citrate buffer, after which nonspecific binding was blocked using 5% BSA. Primary antibodies (diluted 1:100) were incubated overnight at 4°C, and the appropriate secondary antibodies (Alexa Fluor 594–conjugated goat anti-rabbit IgG, 1:1000 dilution; Abcam, Cambridge, MA, USA) were applied for 1 h at room temperature. Finally, slides were mounted with a DAPI-containing medium (Vectashield; Vector Laboratories, Burlingame, CA, USA) and examined under both bright-field and fluorescence microscopy.

Urodynamic study

To evaluate bladder function under conscious conditions, six rats from each group underwent cystometric analysis at 3, 7, and 14 days following implantation of the polyethylene-50 catheter. Prior to measurements, the animals were practiced to the testing room to minimize stress and were then gently restrained without the use of anesthesia to preserve physiological voiding reflexes. The externalized polyethylene-50 tube was connected to a calibrated pressure transducer, and sterile saline maintained at room temperature was infused at a constant rate of 200 μL/min via a syringe pump. Intravesical pressure responses were continuously monitored and recorded using the PowerLab® data acquisition system (AD Instruments Pty., Ltd., Bella Vista, NSW, Australia), which allowed real-time pressure tracing and subsequent quantitative analysis of bladder activity.

Statistical analysis

Data are expressed as mean ± standard deviation (SD). Statistically significant differences were assessed using a t-test and one-way analysis of variance with Tukey's post hoc test. A P-value < 0.05 was considered statistically significant.

Results

Expression patterns of myogenic and neurogenic markers

We analyzed the expression changes of muscle regeneration-related markers, including Pax7, MyoD, Myogenin, and Mef2 (Fig. 1A). In the PNI group, Pax7 and Myogenin were significantly decreased, whereas treatment with Cell + PL showed the greatest recovery among all treatment groups. Pax7 expression was increased in the PNI+Cell and PNI + PL groups, but the increase was more pronounced in the PNI+Cell + PL group, suggesting an enhanced regenerative effect of the combined treatment. Similarly, Myogenin expression gradually recovered following treatment and was highest in the PNI+Cell + PL group, indicating improved myogenic differentiation and maturation. Although Mef2 expression was decreased in the PNI group compared with the control, treatment with PL alone or in combination with cells increased its expression, with the highest level observed in the PNI+Cell + PL group. While some comparisons did not reach statistical significance, the consistent trend toward increased expression suggests that combined Cell + PL treatment may exert superior regenerative effects compared with either treatment alone. In contrast, MyoD, a marker reflecting satellite cell activation and early differentiation, was significantly increased in the PNI group, likely due to denervation-induced regenerative activation. Following treatment, MyoD expression decreased toward control levels, with the PNI+Cell + PL group showing the most normalized expression pattern, suggesting improved stabilization of the regenerative process. These findings suggest that combined Cell + PL treatment more effectively modulates satellite cell activation and differentiation after nerve injury, thereby promoting muscle regeneration and stabilization.

We analyzed the expressions of neural regeneration-related markers, including GFAP, Neurofilament, β-Tubulin III, and MAP2 (Fig. 1B). GFAP and Neurofilament were significantly decreased in the PNI group but recovered following treatment, with the greatest increase observed in the PNI+Cell + PL group. β-Tubulin III also decreased in the PNI group and subsequently increased after treatment, particularly in the combined Cell + PL group, indicating enhanced neural recovery. MAP2 expression was reduced in the PNI group and progressively increased in the treatment groups, with the highest expression again observed in the PNI+Cell + PL group. Although several comparisons between the treatment groups were not statistically significant, the overall expression patterns consistently demonstrated superior recovery in the combined treatment group compared with the Cell-only or PL-only groups. These findings suggest that Cell + PL combination therapy may synergistically promote the recovery of glial cells and neural fibers after nerve injury.

Assessment of leak point pressure (LPP) and closing pressure (CP) measurements

To evaluate urethral sphincter function, LPP and CP were measured using UDS at days 3, 7, and 14 after treatment. In the PNI group, both LPP and CP were markedly decreased compared with the control group throughout the experimental period, indicating impaired urethral sphincter function following pudendal nerve injury. In contrast, treatment groups showed progressive functional recovery over time. Among the treatment groups, the PNI+Cell + PL group demonstrated the greatest improvement in both LPP and CP values, particularly at day 14, suggesting superior restoration of urethral sphincter function by the combined therapy. Although the PNI+Cell + PL group consistently showed the highest functional recovery among the treatment groups, no statistically significant differences were observed compared with the PNI + PL group. The PNI+Cell and PNI + PL groups also exhibited increased LPP and CP values compared with the PNI group, indicating partial functional recovery. Although some comparisons between the treatment groups did not reach statistical significance, the combined Cell + PL treatment consistently showed higher functional values than either Cell or PL treatment alone. These findings suggest that Cell + PL combination therapy more effectively alleviates sphincter dysfunction caused by nerve injury and promotes restoration of bladder outlet resistance. The exact values and statistical significance are presented in Table 2.

Table 2
LPP and CP measurements (cm H_2O)

Group	Day 3		Day 7		Day 14	
	LPP	CP	LPP	CP	LPP	CP
Ctrl	67.75 ± 5.63	48.74 ± 9.48	65.70 ± 11.28	41.94 ± 9.90	65.15 ± 0.91	54.43 ± 4.46
PNI	33.89 ± 8.74 $^{\#\#\#}$	25.12 ± 8.52 $^{\#\#}$	42.87 ± 4.36 $^{\#}$	14.03 ± 0.56 $^{\#\#}$	41.10 ± 8.08 $^{\#\#}$	32.98 ± 4.73 $^{\#\#\#}$
PNI+Cell	43.80 ± 14.58	27.02 ± 4.98	47.91 ± 16.00	28.69 ± 20.01	56.23 ± 6.08 *	28.07 ± 14.40
PNI + PL	47.11 ± 10.20 *	31.89 ± 12.03	51.48 ± 13.31	33.16 ± 4.42 **	57.83 ± 17.90	33.76 ± 6.19
PNI+Cell + PL	58.95 ± 9.08 ***	37.86 ± 6.72 *,§	60.82 ± 10.32 *	29.45 ± 7.55 *	72.53 ± 6.14 **,§§	41.02 ± 11.67

Values are presented as mean ± SD. $^{\#}p < 0.05$, $^{\#\#}p < 0.01$, $^{\#\#\#}p < 0.001$ vs Ctrl; $^{*}p < 0.05$, $^{**}p < 0.01$, $^{***}p < 0.001$ vs PNI; $^{\S}p < 0.05$, $^{\S\S}p < 0.01$, $^{\S\S\S}p < 0.001$ vs PNI+Cell.

Histological assessment of urethral sphincter

After confirming the functional recovery of the urethral sphincter, H&E staining was performed to evaluate histological changes, including muscle fiber organization, inflammatory cell infiltration, and tissue architecture (Fig. 2A). The PNI group exhibited disrupted tissue structure, inflammatory cell infiltration, and degenerative changes compared with the control group. In contrast, the treatment groups showed partial restoration of tissue architecture and reduced inflammatory changes. Among the treatment groups, the PNI+Cell + PL group demonstrated the most preserved tissue morphology and the greatest reduction in inflammatory cell infiltration, suggesting enhanced tissue recovery following combined treatment. Although the PNI+Cell and PNI + PL groups also showed histological improvement compared with the PNI group, the combined Cell + PL group consistently exhibited more normalized histological features.

In addition, Masson's trichrome (MT) staining was conducted to assess collagen deposition and fibrosis (Fig. 2B). The PNI group showed increased collagen accumulation and fibrotic changes compared with the control group. In contrast, collagen deposition was reduced in the treatment groups, particularly in the PNI+Cell + PL group, which exhibited the lowest degree of fibrosis among the injured groups. Although the differences between the PNI + PL and PNI+Cell + PL groups were not clearly distinguishable histologically, the overall staining patterns suggested that combined Cell + PL treatment may provide greater anti-fibrotic and tissue-protective effects than either treatment alone. These findings suggest that Cell + PL combination therapy promotes structural recovery and attenuates fibrosis following pudendal nerve injury.

Immunohistochemical expression of neural and muscle markers

Although only modest changes were observed in conventional histological staining, immunofluorescence staining was performed to further evaluate the expression and localization of muscle- and nerve-related proteins, including nAChRα1, α-SMA, and neurofilament (Fig. 3). For nAChRα1 (Fig. 3A), the control group showed relatively localized positive signals, whereas the PNI group exhibited altered and reduced staining patterns, suggesting disruption of neuromuscular junction-associated protein expression after pudendal nerve injury. In the treatment groups, nAChRα1-positive signals were partially restored, with the PNI+Cell + PL group showing more prominent and organized staining than the Cell- or PL-only groups, indicating improved recovery of neuromuscular junction-related features following combined treatment.

α-SMA staining was performed to assess smooth muscle and sphincter-associated muscle integrity (Fig. 3B). Compared with the control group, the PNI group showed reduced and disorganized α-SMA expression, reflecting muscle injury and impaired sphincter structure. In contrast, α-SMA expression was increased in the treatment groups, particularly in the PNI+Cell + PL group, which showed stronger and more organized α-SMA-positive areas compared with the PNI+Cell and PNI + PL groups. These findings suggest that combined Cell + PL treatment may more effectively promote structural recovery of urethral sphincter muscle after nerve injury.

Neurofilament staining was used to evaluate neural fiber preservation and regeneration (Fig. 3C). The PNI group showed decreased neurofilament-positive signals compared with the control group, indicating nerve fiber damage following pudendal nerve injury. Treatment with Cell or PL alone partially restored neurofilament expression; however, the PNI+Cell + PL group exhibited more evident neurofilament-positive staining, suggesting enhanced neural recovery by the combined therapy. Collectively, these findings indicate that Cell + PL combination therapy may promote both muscular and neural restoration after pudendal nerve injury, with greater recovery patterns than either Cell or PL treatment alone.

Discussion

The present study demonstrates that the combined periurethral injection of USCs and PL significantly enhances structural and functional recovery in a rat model of PNI-induced SUI. While monotherapy with either USCs or PL provided partial therapeutic benefits, the combined treatment group (PNI+Cell + PL) exhibited superior outcomes across all measured parameters, including urodynamic pressure profiles, histological tissue architecture, mitigation of fibrosis, and the molecular restoration of both myogenic and neurogenic markers. Our findings are organized around three principal observations: (1) PNI significantly suppressed myogenic regulatory factors (Pax7, myogenin, Mef2) and neural integrity markers (GFAP, neurofilament, β-tubulin III, MAP2) while acutely upregulating the early myogenic activation marker MyoD; (2) Cell + PL combination therapy most effectively restored these molecular markers, reduced fibrotic collagen deposition, and recovered α-SMA and nAChRα1 expression; and (3) urethral sphincter function, as measured by LPP and CP, was most substantially improved in the Cell + PL group, achieving statistically significant recovery relative to both the PNI and PNI+Cell groups, particularly at day 14. Collectively, these results support the concept that combining viable stem cells with a growth factor–enriched acellular biologic creates a therapeutic synergism capable of addressing the multidimensional pathology of PNI-induced sphincter dysfunction.

The myogenic response to PNI observed in the present study follows a well-characterized pattern of denervation-induced muscle remodeling. The acute upregulation of MyoD in the PNI group is consistent with the known role of this myogenic regulatory factor as an early marker of satellite cell activation in response to denervation, reflecting an attempt at compensatory myogenic repair [15]. However, the concurrent downregulation of Pax7, myogenin, and Mef2 indicates that this regenerative response remains incomplete. Pax7 is essential for the self-renewal and maintenance of the satellite cell pool; its reduction implies progressive depletion of the muscle progenitor reserve following chronic denervation [16]. Myogenin and Mef2 govern the late stages of myogenic differentiation—myoblast fusion and maturation into contractile myotubes—and their suppression therefore represents a failure to execute terminal myogenic commitment [17]. The PNI+Cell + PL group showed the greatest normalization of this myogenic cascade, with Pax7 and myogenin recovering toward control levels. This pattern suggests that PL-derived growth factors—particularly IGF-1 and HGF—may activate the Pax7–myogenin axis in resident satellite cells and transplanted USCs, while USCs themselves provide paracrine support that sustains satellite cell commitment through secretion of cytokines such as IL-6 and leukemia inhibitory factor (LIF) [18,19]. The concomitant normalization of MyoD toward control levels in the Cell + PL group suggests

that improved downstream differentiation reduces the demand for continued early progenitor activation, consistent with a model of restored myogenic homeostasis.

The recovery of neural markers in the Cell + PL group provides compelling evidence for a neuroprotective and neuroregenerative component of the combined therapy. GFAP upregulation, which was most prominent in the Cell + PL group, reflects activation and proliferation of Schwann cells and other glial supportive elements essential for peripheral nerve regeneration [20]. Schwann cell–mediated remyelination and axonal guidance are critical determinants of functional recovery following peripheral nerve injury, and their activation by PL-derived PDGF and VEGF has been documented in peripheral nerve repair models [21]. Neurofilament and β-tubulin III—structural components of axonal cytoskeleton—were progressively restored across the treatment groups, with the highest recovery in the Cell + PL group, indicating regeneration and/or preservation of intra-sphincteric nerve fibers. MAP2, a marker of dendritic integrity and mature neural differentiation, similarly recovered in the Cell + PL group, suggesting restoration of the synaptic organization necessary for coordinated sphincter neuromuscular control [22]. These effects are mechanistically supported by the known neurotrophin-like properties of PL growth factors—including NGF and BDNF—which promote neuronal survival and axonal elongation—as well as by the documented capacity of USCs to secrete GDNF, NGF, and BDNF in vivo, creating a local neurotrophic gradient that sustains neural recovery [7,23]. Immunofluorescence data further confirmed that neurofilament-positive staining was most prominent in the Cell + PL group, providing spatial confirmation of neural fiber preservation in the sphincter tissue.

The restoration of α-SMA expression and the attenuation of collagen deposition in the treatment groups —most pronounced in the Cell + PL group—reflect recovery of smooth muscle contractile phenotype and anti-fibrotic remodeling. Denervation-induced phenotypic switching of smooth muscle cells from a contractile to a synthetic state, associated with downregulation of α-SMA and upregulation of collagen synthesis, is a central pathological mechanism in chronic sphincter dysfunction [24]. PL-derived TGF-β1 exerts context-dependent effects on smooth muscle: while it can promote fibrosis at high concentrations, at physiological levels it supports smooth muscle differentiation in combination with appropriate myogenic stimuli [25]. The Cell + PL group's enhanced α-SMA recovery may therefore reflect a balanced interaction in which PL provides myogenic differentiation cues while USCs counteract fibrogenic signaling through secretion of anti-fibrotic mediators such as prostaglandin E2 and hepatocyte growth factor [26, 27]. The immunofluorescence data for nAChRα1 further support structural recovery of the neuromuscular junction in the Cell + PL group, with stronger and more organized nAChRα1-positive staining compared with monotherapy groups. Restoration of nAChRα1 at the neuromuscular junction is functionally significant, as its re-expression and correct localization are required for effective acetylcholine-mediated neuromuscular transmission and sphincter contraction [28].

Since functional restoration of the EUS is the ultimate goal of regenerative therapy for SUI, the urodynamic data are the most direct measure of functional recovery in the present study. Both LPP and CP were markedly reduced in the PNI group throughout the observation period, confirming successful

surgical induction of sphincter incompetence. The PNI+Cell + PL group demonstrated statistically significant improvement in LPP compared with the PNI group at all time points and surpassed the PNI+Cell group at days 3 and 14, achieving LPP values that were not statistically different from control by day 14. This pattern of functional recovery is consistent with the molecular and histological data, and supports the interpretation that Cell + PL combination therapy addresses both the neural and muscular components of sphincter dysfunction with a degree of efficacy not achievable by either treatment in isolation. The observation that the PNI + PL group showed numerically comparable LPP improvement to the PNI+Cell + PL group at day 14—without reaching statistical significance between the two groups—raises the possibility that PL alone provides substantial early trophic support, and that the additional benefit of USCs may be most apparent under conditions of more severe or chronic injury [29]. This temporal complementarity between rapid PL-mediated trophic effects and sustained USC-mediated regeneration warrants further investigation. Notably, the lack of statistical significance in CP comparisons between some groups may reflect the greater variability inherent in measuring passive urethral closure properties compared with LPP, and larger sample sizes may be needed to detect differences in this parameter.

Despite these highly promising results, several limitations must be acknowledged. First, the 14-day evaluation period captures the subacute phase of regeneration. While this timeframe is appropriate for evaluating molecular and early functional changes, long-term studies (e.g., 8 to 12 weeks) are required to confirm the durability of the functional recovery and the long-term survival and fate of the engrafted USCs. Second, while we utilized a standardized PL preparation, the exact concentration of individual cytokines and their distinct mechanistic contributions to USC differentiation were not quantified. Third, the mechanisms underlying USC–PL synergism were not directly interrogated at the molecular level; future studies incorporating USC-conditioned medium proteomics, co-culture assays, and pathway inhibitor experiments would clarify the relative contributions of paracrine, direct cellular, and growth factor–mediated mechanisms.

From a translational perspective, the Cell + PL strategy evaluated in the present study possesses several attributes that favor clinical development. USCs can be obtained non-invasively from a patient's own voided urine, eliminating the procedural risks and ethical concerns associated with bone marrow aspiration or adipose tissue harvest for autologous cell therapy [5, 30]. Platelet lysate derived from expired platelet concentrates represents a scalable, economical, and ethically acceptable growth factor source with an established safety record in clinical transfusion medicine and an emerging role as a GMP-compliant cell culture supplement [12]. The periurethral injection route employed in the present study is already in clinical use for bulking agent delivery in SUI, providing an accessible delivery platform for combined USC + PL therapy [31]. Taken together, these considerations position the USC + PL combination as a clinically feasible and scientifically compelling approach to the regenerative treatment of PNI-associated urinary incontinence, pending optimization in large-animal models and formal safety/efficacy evaluation in human trials.

Conclusions

This study demonstrates that the combined application of USCs and PL synergistically promotes the structural and functional regeneration of the EUS in a rat model of PNI. The co-administration significantly improved urodynamic parameters (LPP and CP), restored the morphological integrity of the neuromuscular junction, and up-regulated key molecular markers of both myogenesis and neurogenesis while effectively suppressing denervation-induced fibrosis. By utilizing PL to optimize the hostile host microenvironment, this combinatory approach maximizes the regenerative potential of USCs, offering a highly accessible, minimally invasive, and promising therapeutic strategy for the clinical management of SUI.

Declarations

Ethics approval and consent to participate

All procedures were performed in accordance with the Guide for the Care and Use of Laboratory Animals. The animal study entitled “Urethral Sphincter Regeneration Using Expired Platelet-Derived Extracts and Stem Cells” was approved by the Institutional Animal Care and Use Committee of Yeungnam University Medical Center (Approval No. YUMC-AEC2024-010; approved on May 1, 2024).

Consent for publication

Not applicable. The manuscript does not contain any identifiable individual patient data.

Competing Interests

The authors have declared that no competing interest exists.

Funding

This research was supported by a grant from the Korea Health Technology R&D Project through the Korea Health Industry Development Institute (KHIDI), funded by the Ministry of Health & Welfare, Republic of Korea (RS-2022-KH130593) and the Korea Medical Device Development Fund grant funded by the Korea government (the Ministry of Science and ICT, the Ministry of Trade, Industry and Energy, the Ministry of Health & Welfare, and the Ministry of Food and Drug Safety) (Project Number: 2410018879, RS-2026-25545758), and by the InnoCORE program of the Ministry of Science and ICT(26-InnoCORE-02).

Author Contribution

E.H.L.: Data curation, Investigation, Writing – original draft. M.J.: Investigation, Resources. J.K.: Investigation, Validation. J.C.: Data curation, Visualization. Y.H.: Investigation, Software, Formal analysis. P.H.S.: Investigation, Methodology, Supervision. M.H.: Investigation, Formal analysis, Visualization.

T.G.K.: Data curation, Methodology, Supervision. B.S.K.: Conceptualization, Funding acquisition, Methodology, Project administration, Writing – review & editing.

Acknowledgments

The authors declare that they have not used AI-generated work in this manuscript..

Data availability

The data supporting the findings of this study are available from the corresponding author upon reasonable request. The data are securely stored in the authors' research notes and institutional research database.

References

1. Abrams P, Cardozo L, Fall M, The standardisation of terminology of lower urinary tract function: report from the, Standardisation Sub-committee of the International Continence Society. Neurourol Urodyn, Novara G, Artibani W, Barber MD, Updated systematic review and meta-analysis of the comparative data on colposuspensions, pubovaginal slings, and midurethral tapes in the surgical treatment of female stress urinary incontinence. Eur Urol. 2010;58:218 – 38. https://doi: 10.1016/j.eururo.2010.04.022. 3., Ford AA, Rogerson L, Cody JD, Aluko P, Ogah JA. Mid-urethral sling operations for stress urinary incontinence in women. Cochrane Database Syst Rev. 2017;7:CD006375., Liu X, Li T, Zhang J, Mesehcnymal stem cell-based therapy for female stress urinary incontinence. Front Cell Dev Biol. 2023;11:1007703. https://doi: 10.3389/fcell.2023.1007703. 5., Zhang Y, McNeill E, Tian H, Urine derived cells are a potential source for urological tissue reconstruction. J Urol. 2008;180:2226-33. https://doi: 10.1016/j.juro.2008.07.023. 6., Bharadwaj S, Liu G, Shi Y, Multipotential differentiation of human urine-derived stem cells: potential for therapeutic applications in urology. Stem Cells. 2013;31:1840-56. https://doi: 10.1002/stem.1424. 7., Liu G, Pareta RA, Wu R, Skeletal myogenic differentiation of urine-derived stem cells and angiogenesis using microbeads loaded with growth factors. Biomaterials. 2013;34:1311–26. https://doi: 10.1016/j.biomaterials.2012.10.038. 8., Tasso R, Augello A, Boccardo S, Recruitment of a host's osteoprogenitor cells using exogenous mesenchymal stem cells seeded on porous ceramic. Tissue Eng Part A. 2009;15:2203–12., Williams AR, Hare JM. Mesenchymal stem cells: biology, pathophysiology, translational findings, and therapeutic implications for cardiac disease. Circ Res. 2011;109:923 – 40. https://doi: 10.1161/CIRCRESAHA.111.243147. 10. Doucet C, Ernou I, Zhang Y, Platelet lysates promote mesenchymal stem cell expansion: a safety substitute for animal serum in cell-based therapy applications. J Cell Physiol. 2005;205:228 – 36. https://doi: 10.1002/jcp.20391. 11., Astori G, Amati E, Bambi F, Platelet lysate as a substitute for animal serum for the ex-vivo expansion of mesenchymal stem/stromal cells: present and future. Stem Cell Res Ther. 2016;7:93. https://doi: 10.1186/s13287-016-0352-x. 12. Bieback K. Platelet lysate as replacement for fetal

bovine serum in mesenchymal stromal cell cultures. Transfus Med Hemother. 2013;40:326–35. https://doi: 10.1159/000354061. 13., Fitzpatrick J, Bulsara MK, McCrory PR, Richardson MD, Zheng MH. Analysis of platelet-rich plasma extraction: variations in platelet and blood components between 4 common commercial kits. Orthop J Sports Med. 2017;5:2325967116675272. https://doi: 10.1177/2325967116675272. 14. Perez AG, Rodrigues AA, Luzo AC, Lana JF, Belangero WD, Santana MH et al. Fibrin network architectures in pure platelet-rich plasma as characterized by fiber radius and correlated with clotting time. J Mater Sci Mater Med. 2014;25:1967–77. https://doi:10.1007/s10856-014-5235-z.

2. Grounds MD. Towards understanding skeletal muscle regeneration. Pathol Res Pract. 1991;187:1–22. https://doi:10.1016/S0344-0338(11)81039-3.
3. Zammit PS, Golding JP, Nagata Y, Hudon V, Partridge TA, Beauchamp JR. Muscle satellite cells adopt divergent fates: a mechanism for self-renewal? J Cell Biol. 2004;166:347–57. https://doi:10.1083/jcb.200312007.
4. Molkentin JD, Olson EN. Defining the regulatory networks for muscle development. Curr Opin Genet Dev. 1996;6:445–53. https://doi:10.1016/s0959-437x(96)80066-9.
5. Sheehan SM, Tatsumi R, Temm-Grove CJ, Allen RE. HGF is an autocrine growth factor for skeletal muscle satellite cells in vitro. Muscle Nerve. 2000;23:239–45. 10.1002/(sici)1097-4598(200002)23:2%3C239::aid-mus15%3E3.0.co;2-u. https://.
6. Tran C, Damaser MS. Stem cells as drug delivery methods: application of stem cell secretome for regeneration. Adv Drug Deliv Rev. 2015;82–83:1–11. https://doi:10.1016/j.addr.2014.10.007.
7. Sofroniew MV, Vinters HV. Astrocytes: biology and pathology. Acta Neuropathol. 2010;119:7–35. https://doi:10.1007/s00401-009-0619-8.
8. Gordon T. The role of neurotrophic factors in nerve regeneration. Neurosurg Focus. 2009;26:E3. 10.3171/FOC.2009.26.2.E3. https://doi.
9. Dehmelt L, Halpain S. The MAP2/Tau family of microtubule-associated proteins. Genome Biol. 2005;6:204. https://doi:10.1186/gb-2004-6-1-204.
10. Thoenen H. Neurotrophins and neuronal plasticity. Science. 1995;270:593–8. https://doi:10.1126/science.270.5236.593.
11. Andersson KE, Arner A. Urinary bladder contraction and relaxation: physiology and pathophysiology. Physiol Rev. 2004;84:935–86. https://doi:10.1152/physrev.00038.2003.
12. Kalluri R, Neilson EG. Epithelial-mesenchymal transition and its implications for fibrosis. J Clin Invest. 2003;112:1776–84. https://doi:10.1172/JCI20530.
13. Aguilar S, Nye E, Chan J, et al. Murine but not human mesenchymal stem cells generate osteosarcoma-like lesions in the lung. Stem Cells. 2007;25:1586–94. https://doi:10.1634/stemcells.2006-0762.
14. Li T, Xia M, Gao Y, Chen Y, Xu Y. Human umbilical cord mesenchymal stem cells: an overview of their potential in cell-based therapy. Expert Opin Biol Ther. 2015;15:1293–306. https://doi:10.1517/14712598.2015.1051528.

15. Bhatt DL, Topol EJ. Scientific and therapeutic advances in antiplatelet therapy. Nat Rev Drug Discov. 2003;2:15–28. https://doi:10.1038/nrd985.
16. Spees JL, Lee RH, Gregory CA. Mechanisms of mesenchymal stem/stromal cell function. Stem Cell Res Ther. 2016;7:125. https://doi:10.1186/s13287-016-0363-7.
17. Bharadwaj S, Liu G, Shi Y, et al. Characterization of urine-derived stem cells obtained from upper urinary tract for use in cell-based urological tissue engineering. Tissue Eng Part A. 2011;17:2123–32. https://doi:10.1089/ten.TEA.2010.0637.
18. Kirchin V, Page T, Keegan PE, Atiemo K, Cody JD, McClinton S. Urethral injection therapy for urinary incontinence in women. Cochrane Database Syst Rev. 2012;15:CD003881. https://doi:10.1002/14651858.CD003881.pub4.

Figures

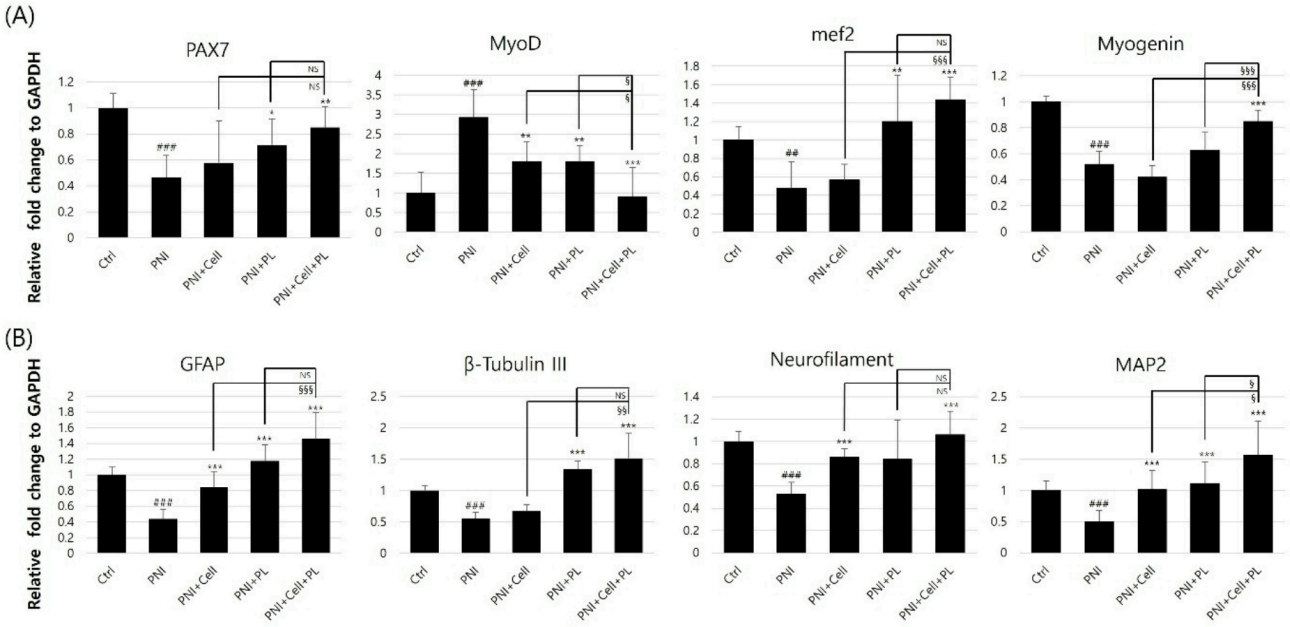


Figure 1

Gene expression changes of (A) myogenic and (B) neuronal markers. Data are presented as the mean ± SD from three independent experiments. Statistical significance: $p < 0.05$, ##$p < 0.01$, ###$p < 0.001$; Ctrl vs. PNI; *$p < 0.05$, **$p < 0.01$, ***$p < 0.001$; PNI vs. PNI+Cell.

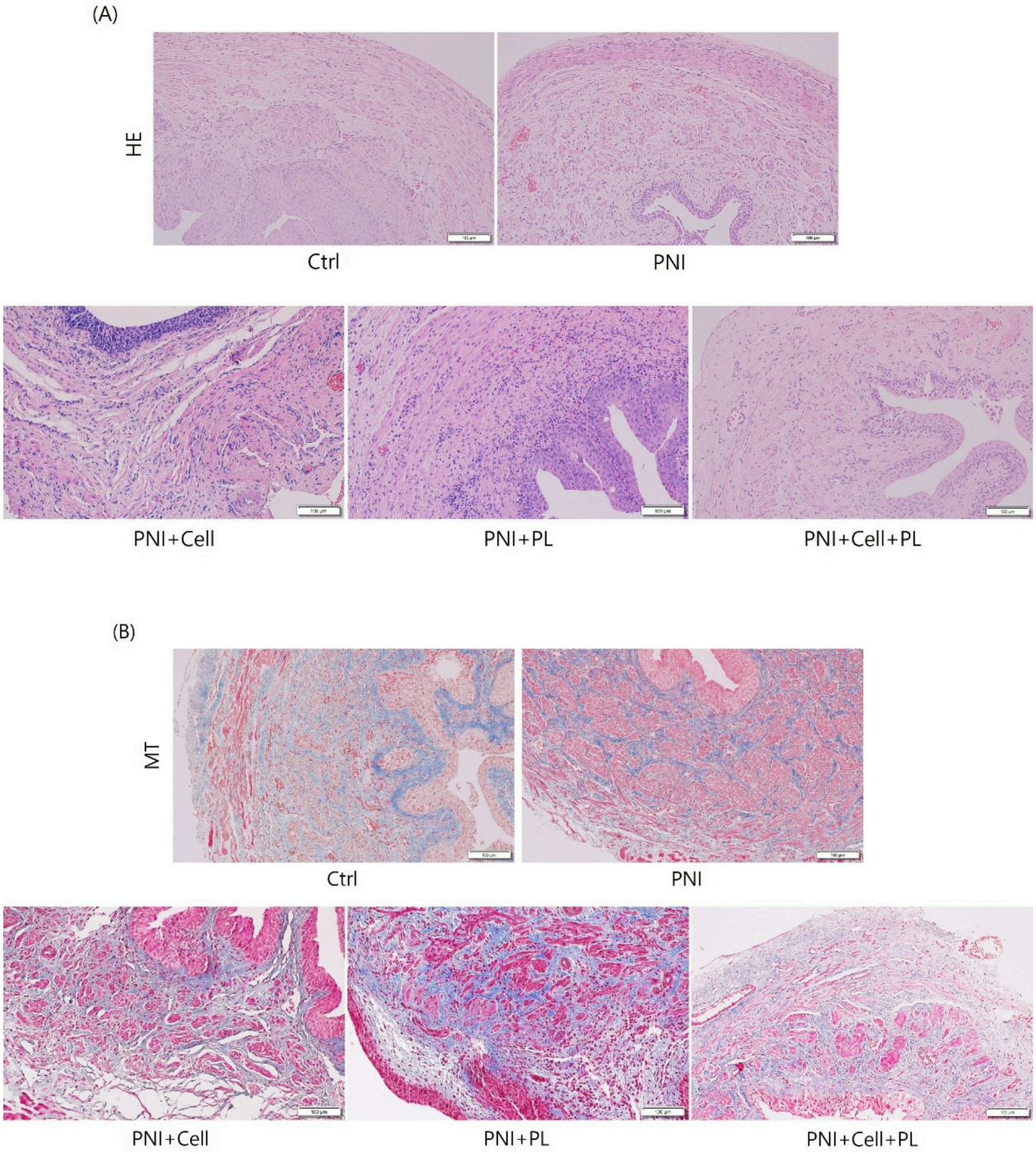


Figure 2

Hematoxylin and eosin staining (A) and Masson's trichrome staining (B) of the urethral sphincter.

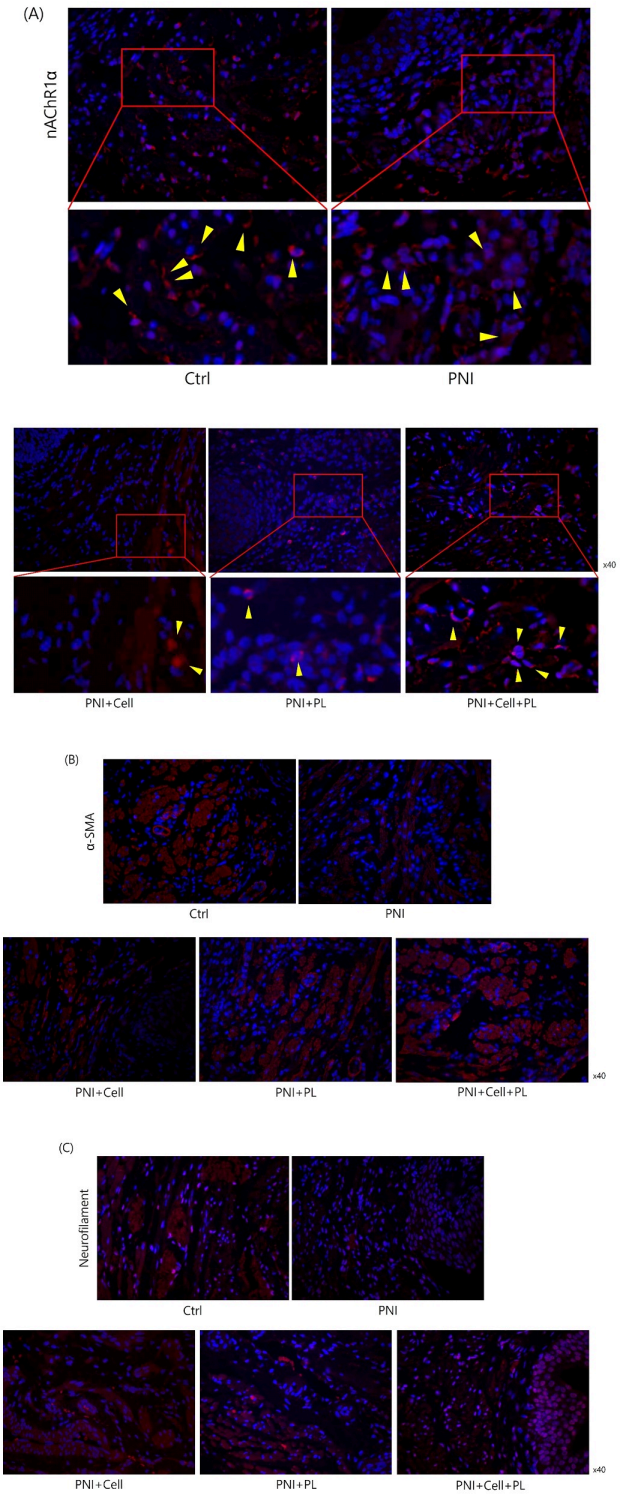


Figure 3

Immunohistochemical (IHC) staining of nicotinic acetylcholine receptor α1 (A), α-SMA (B), and neurofilament (C).